

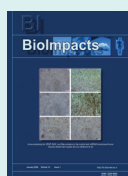


# Bioscaffolds of graphene based-polymeric hybrid materials for myocardial tissue engineering

Nazanin Amiryaghoubi<sup>1</sup>, Marziyeh Fathi<sup>1\*</sup>

Research Center for Pharmaceutical Nanotechnology, Biomedicine Institute, Tabriz University of Medical Sciences, Tabriz, Iran

## Article Info



**Article Type:**  
Review

### Article History:

Received: 7 Nov. 2022  
 Revised: 20 May 2023  
 Accepted: 3 Jul. 2023  
 ePublished: 12 Aug. 2023

### Keywords:

Biomaterials,  
 Cardiac vascular,  
 Graphene-polymer  
 bioscaffolds,  
 Tissue engineering

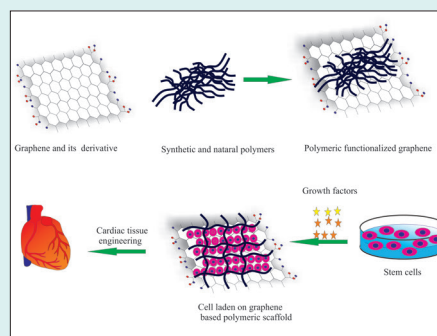
## Abstract

**Introduction:** Biomaterials currently utilized for the regeneration of myocardial tissue seem to associate with certain restrictions, including deficiency of electrical conductivity and sufficient mechanical strength. These two factors play an important role in cardiac tissue engineering and regeneration. The contractile property of cardiomyocytes depends on directed signal transmission over the electroconductive systems that happen inside the innate myocardium. Because of their distinctive electrical behavior, electroactive materials such as graphene might be used for the regeneration of cardiac tissue.

**Methods:** In this review, we aim to provide deep insight into the applications of graphene and graphene derivative-based hybrid polymeric scaffolds in cardiomyogenic differentiation and cardiac tissue regeneration.

**Results:** Synthetic biodegradable polymers are considered as a platform because their degradation can be controlled over time and easily functionalized. Therefore, graphene-polymeric hybrid scaffolds with anisotropic electrical behavior can be utilized to produce organizational and efficient constructs for macroscopic cardiac tissue engineering. In cardiac tissue regeneration, natural polymer based-scaffolds such as chitosan, gelatin, and cellulose can provide a permissive setting significantly supporting the differentiation and growth of the human induced pluripotent stem cells -derived cardiomyocytes, in large part due to their negligible immunogenicity and suitable biodegradability.

**Conclusion:** Cardiac tissue regeneration characteristically utilizes an extracellular matrix (scaffold), cells, and growth factors that enhance cell adhesion, growth, and cardiogenic differentiation. From the various evaluated electroactive polymeric scaffolds for cardiac tissue regeneration in the past decade, graphene and its derivatives-based materials can be utilized efficiently for cardiac tissue engineering.



## Introduction

Myocardial infarction (MI) often occurs due to the disruption in the coronary blood supply to the myocardium tissue and induces irreversible myocardial damage.<sup>1</sup> The myocardium, the so-called cardiac muscle tissue, holds specialized cells that are responsible for the rhythmic expansion and contraction in association with the neural electrical impulses. Such an immaculate function of the myocardium makes the regeneration of myocardial tissue extremely challenging. Further, the cardiac muscle tissue has a restricted capability of restoration. Consequently, transplantation is the

main solution despite being associated with numerous difficulties. Hence, myocardial tissue regeneration might be one of the most effective treatment modalities for restoring cardiac functions.<sup>2</sup> Cardiac tissue engineering should ideally result in the production of efficient tissue constructs with desired physiological functions of the natural cardiac muscle tissue to restore/rejuvenate the injured tissues.<sup>3,4</sup> Cardiomyocytes and fibroblasts are the two types of cells in the myocardium. In the myocardium, scatters of fibroblasts are among cardiomyocytes along with extracellular matrix (ECM) in association with blood and lymphatic vessels together with nerve endings. In such a



\*Corresponding author: Marziyeh Fathi, Email: fathi.marziyeh@yahoo.com, fathim@tbzmed.ac.ir



© 2024 The Author(s). This work is published by BioImpacts as an open access article distributed under the terms of the Creative Commons Attribution Non-Commercial License (<http://creativecommons.org/licenses/by-nc/4.0/>). Non-commercial uses of the work are permitted, provided the original work is properly cited.

complex microstructure, cardiomyocytes play a key role in forming the myocardial tissue.<sup>5</sup> In the tissue regeneration process, the scaffold plays a pivotal role in the safe delivery of the incorporated cells and necessary substances such as growth factors. To improve the regenerative ability of stem cells and biological properties, the scaffold should possess desirable elasticity, stiffness, and topography.<sup>6</sup> Graphene (GR) has been used as a scaffold (i.e., in cell differentiation, proliferation, adherence, and healing processes) because of its high biocompatibility, nontoxic biodegradation, large surface area, excellent electrical conductivity, suitable mechanical strength, stiffness, high elasticity, low toxicity, flexibility, and unique thermal properties.<sup>7-10</sup> To create new hybrid scaffolds for enhanced tissue engineering, GR can be functionalized with different types of biomacromolecules such as DNA, proteins, peptides, enzymes, and polymers.<sup>11-13</sup> It has been shown that the reinforcement of a biopolymer or a synthetic polymer with GR and GR-derived products can enhance the wettability as well as the antibacterial activity of scaffolds.<sup>14,15</sup> It also improves its biocompatibility, mechanical, and electrical properties. The integration of biopolymers with GR can result in the development of electroconductive biocompatible scaffolds with functional entities (e.g., amine, carboxyl, and hydroxyl groups). Such potential might result in an improved interaction of scaffold with biomacromolecules favoring cellular attachment, proliferation, and differentiation.<sup>16</sup>

#### **Applications and fabrication of graphene and its derivative-based scaffolds by various techniques in cardiac tissue regeneration**

Cardiac tissue involves an extremely complex internal microvasculature setting that contains cardiomyocytes, endothelial cells (ECs), fibroblasts, and pericytes together with ECM.<sup>17</sup> It is an organ with a minimal capacity to play key roles to regenerate in pumping blood and oxygen to other organs, supplying nutrients, and maintaining blood circulation homeostasis.<sup>18</sup> Attributable to its 3D structure, the myocardial tissue provides an aligned synchronized beating pulse, which is largely dependent on the functions of the major fibrous proteins of myocardial ECM (e.g., collagen (Col) types I and III) generated by cardiac fibroblasts and is necessary for the stiffness and structural integrity of cardiac tissue.<sup>19,20</sup> The contractile property and synchronized beating of cardiomyocytes (CMs) are entirely related to cellular orientation, elongation, and anisotropic microarchitecture of cardiac tissue.<sup>21,22</sup> The electrospinning technique provides well-organized and interconnected porous scaffold fibers that can mimic the anisotropic structure of the native myocardium, thus improving the contraction patterns, topographical features, and cellular alignments.<sup>23</sup> Beating pulse rate and electrical transferring properties are related to the electroactivity of cardiac muscle tissue, that is, 0.005 transverse and ~0.1 longitudinal S/m. Heart transplantation for the treatment

of cardiovascular diseases (CD) is often limited mainly due to insufficient allograft tissue for transplantation, immune rejection, surgical complications, and a shortage of donors. Therefore, there is great interest in designing an ideal artificial cardiac scaffold with contractile and electrophysiological properties to be used for cardiac tissue construction and stimulating vasculogenesis.<sup>24,25</sup> In heart disease, such as MI, and endocarditis, different tissues including blood vessels are affected.<sup>26-30</sup> MI can occur due to occlusion of coronary arteries, which results in myocardial ischemia and hence heart dysfunction. Notably, the resultant apoptotic process in cardiomyocytes can alter contractile and electrophysiological characteristics that are responsible for the death of a large number of patients globally.<sup>31,32</sup>

For the treatment of MI, it is necessary to prompt the proliferation of contractile cells. Awada et al showed that the use of stem cells, growth factors, peptides, biomaterials, and inflammatory mediators could regulate the inflammatory response of the heart tissue, promote the proliferation of cardiomyocytes and regenerate the damaged myocardial area.<sup>33,34</sup> Stem cells can differentiate into cardiomyocytes, induce vascularization, and consequently enhance contractile functionality in the injured heart tissue. In the cardiac tissue, there exist two main cell populations, including (i) cardiomyocytes that are responsible for contraction and (ii) fibroblasts that produce ECM proteins and play an important role during MI.<sup>35</sup> It is indicated that the thickness of the left ventricular wall, angiogenesis, and myocardial revascularization have been increased by the rapid infiltration of cardiac fibroblasts. Therefore, these aspects must be considered in tissue engineering in MI. In this area, cardiac tissue engineering (CTE) has been advanced using safe natural or synthetic scaffolds with desired substances. Such tissue engineering modalities can result in the differentiation of stem cells into cardiac cells, which can be used as a substitute for ischemic/infarcted cardiac cells.<sup>36,37</sup> The main principles of CTE should be (i) efficiently improving the contractile and electrophysiological function of the heart muscles, (ii) properly reorganizing cells into tissues, and (iii) substantially regenerating microvasculature networks within a scaffold for the damaged myocardium and vascularization. In CTE, an ideal artificial cardiac scaffold should provide (i) high electrical conductivity for the electrophysiological application, (ii) suitable mechanical stiffness of the native cardiac tissue (anisotropy, elasticity, contractility), (iii) better biological settlement towards fibrous anisotropic alignment like myocardium to stimulate functional vascularization, and (iv) excellent cytocompatibility in terms of cellular behaviors (e.g., proliferation, differentiation) with no/trivial inflammatory responses. Given Young's modulus of the native heart tissue in the range of 10–15 kPa,<sup>38</sup> a scaffold for the heart soft tissue needs to be very flexible with lower tensile strength. Thus, scaffolds based on the

Col fibrous structure of ECM myocardium may serve as an ideal platform for the biological activities of the implanted cells such as migration of cells from the implanted scaffold and differentiation towards angiogenesis for instance. Scaffolds with adequate mechanical properties and high flexibility, such as the myocardial Col are deemed to restore and improve the myocardial contractile performance and regeneration. Likewise, various porous and fibrous scaffolds, as well as hydrogels, have been used to engineer heart valves. Accordingly, solid free-form fabrication has been used to engineer 3D interconnected porous scaffolds with acceptable mechanical strength for tissue regeneration.<sup>39</sup> Given the potential of the quality-by-design micropatterned elastomer film in the simulation of the mechanical properties, anisotropy, and electroactivity of natural myocardial tissues, Shi et al capitalized on poly(glycerol sebacate) (PGS) and graphene (GR) and developed micropatterned elastomeric films.<sup>40</sup> Having appropriate mechanical strength (0.6 +/- 0.1-3.2 +/- 0.08 MPa) to withstand heartbeats, the films displayed satisfactory micropatterned structure to mimic the natural myocardium anisotropy. Furthermore, owing to the GR presence in the films, they showed good conductivity. Both in vitro and in vivo examinations (in H9c2 rat cardiomyocyte cells and rats, respectively) confirmed the biocompatibility and effectiveness of the films, particularly films with 1 wt% GR content (PGS-GR1). Based on the animal model analyses, the PGS-GR1 micropatterned film was found to substantially improve the myocardial functions after MI, resulting in improved function in the myocardium. In the treated rats, the left ventricular internal dimension in systole and diastole showed a meaningful downward trend, while the fractional shortening and ejection fraction were found to be considerably improved. Collectively, such an electroconductive micropatterned elastomer film with desired mechanical and anisotropic properties seems to provide the right scaffold for CTE and regeneration.

#### ***Fabrication of graphene and its derivative scaffolds by a three-dimensional (3D) printing technique***

A 3D printing approach is an advanced form of solid free-form (SFF), which can be used for the production of porous 3D structures from a variety of materials such as natural and synthetic polymers for tissue engineering.<sup>41</sup> This method allows cells to grow, proliferate, and deposit ECM on the fabricated 3D solid porous scaffold for stem cell differentiation into functional tissue constructs. The 3D printing strategy is a rapid prototyping multidisciplinary approach integrating chemistry, optics, and robotics, which is referred to as SFF additive manufacturing to produce 3D layered heterogeneous constructs mimicking native tissue traits. For example, an implementation of the UV-integrated 3D-bioprinting technique was shown to provide a highly uniform structure with unique physiological and biomechanical properties to mimic a

lenient microenvironment similar to that of the native myocardium and cardiac tissue.<sup>42</sup> For example, in a study, a 3D graphene oxide-polyethyleneimine (GO-PEIs) scaffold was prepared for cardiac tissue regeneration. Considering the high reactivity of functional epoxy and edge carboxylate groups of the GO when cooperating, with  $\text{NH}_2$  and  $\text{NH}_3^+$  assemblies of linear PEIs, respectively, 3D constructions could be produced with adjustable width, porosity, enriched compositional, and organizational regulation. The elasticity modulus of the prepared scaffold originated too, reliant on the width of the platform, with the lowest amount of 13 GPa attained in groups comprising the maximum amount of alternating sheets. Because of the amino-rich arrangement of the scaffold and the well-known biocompatibility of GO, the platforms did not display cytotoxicity; they endorsed cardiac muscle HL-1 cell attachment and proliferation without interfering with the cell shape and enhancing cardiac markers for example Connexin-43 and Nkx 2.5. The new approach for scaffold synthesis consequently overwhelmed the drawbacks related to the restricted processability of pure GR and little GO conductivity and allowed the fabrication of biocompatible 3D GO platforms functionalized with amino-grounded spacers, which was beneficial for cardiac tissue regeneration usages. In particular, they indicated a significant increase in the total gap junctions relative to HL-1 cultivated on control substrates, which renders them to main constituents for restoring injured heart organs besides being utilized for 3D in vitro cardiac forming studies.<sup>43</sup>

#### ***Fabrication of fibrous scaffolds based on graphene and its derivative by electrospinning technique***

Fibrous scaffolds are one of the best selections for cell adhesion, nutrient transportation, and differentiation in heart valve tissue engineering, mainly due to (i) their similar morphology to the ECM of the natural tissue, (ii) the high aspect ratio of fibers with high efficiency to growth factor, (iii) anisotropic organization, (iv) high surface-to-volume ratio, (v) porosity and mechanical characteristics necessary for the cell migration and vascularization.<sup>44,45</sup> Electrospinning is one of the techniques to prepare fibrous scaffolds ranging from nanoscale to microscale. In this technique, applying a high electrical voltage generates free charges on the surface of the polymer droplets that repel each other, overcoming surface tension, fluid elasticity, and formation of the liquid jet.<sup>46,47</sup> Because of bending instability and electrostatic forces, the jet accelerates toward the collecting surface and is stretched to become narrower resulting in the production of solid fibers. The GR-based nanocomposites are reflected as unique selections for increasing electrical and mechanical properties in cardiac tissue regeneration. In a study, rGO-silver (rGO-Ag) nanocomposites (1 and 2 wt%) were prepared and assimilated into polyurethane (PU) nanofibers through the electrospinning method.

The mechanical strengths, electrical behavior, and human cardiac progenitor cells (hCPCs) adhesion on the prepared scaffold were enhanced. The tensile strength, wettability, and electrical conductivity of PU nanofibers were significantly increased after incorporation with rGO-Ag nanocomposites. Real-time polymerase chain reaction (PCR) indicated the enhanced expression of cardiac precise genes containing GATA-4, T-box 18 (TBX 18), cardiac troponin T (cTnT), and alpha-myosin heavy chain ( $\alpha$ -MHC) in the PU/rGO-Ag platforms as relative to pure PU samples. Consequently, prepared nanofibrous rGO-Ag-strengthened PU platforms could be reflected as appropriate applicants in cardiac tissue regeneration.<sup>48</sup> Fakhrli et al fabricated poly(caprolactone)/Gel (PCL/Gel) nanofibrous platforms and GO (GO 0.3, 0.6, and 1% w/w) was assimilated into scaffolds. The diameter of PCL nanofibers was improved by the incorporation of Gel and GO, particularly by the addition of 1 %w/w of GO ( $210 \pm 20$  nm against  $482 \pm 104$  nm). Mechanical strengths and hydrophilicity were enhanced, too. All groups were biocompatible and the highest viability values attained approximately  $91.71 \pm 0.1\%$  and  $94.29 \pm 1.1\%$ , which were related to PCL/Gel and PCL/Gel/GO<sub>0.3</sub>, respectively.<sup>49</sup>

#### **Fabrication of hydrogel scaffolds based on graphene and its derivative**

Hydrogel scaffolds offer higher cell adhesion, proliferation, and differentiation for heart valve engineering primarily due to (i) high water content,<sup>50</sup> (ii) mimicking the structure of proteins and other biomolecule chains similar to the native ECM,<sup>51-53</sup> (iii) high permeability to oxygen, nutrients, the hydrophilic polymer, and (iv) sufficient affinity to growth factor delivery. Hydrogels can act as a carrier for growth factors and induce angiogenesis in ischemic tissues. Hydrogels are ideal candidates to form interconnected networks similar to that of the native microvasculature. Further, porous hydrogels with oxygen-releasing groups promote the vascularization or direct alignment of cardiac cells and prevent cell hypoxia in the ischemic myocardium, improving cardiac function.<sup>54</sup> Conductive hydrogels restore the electrophysiological functions of the cardiomyocytes and stimulate the synchronous beating behavior of the heart. Besides, elastic hydrogels provide flexibility and a dynamic environment for the expansion and contraction of the muscle heart. Altogether, it can be assumed that elastomeric and conductive hydrogels with oxygen-releasing and vasculogenic potential might serve as an excellent scaffold to generate functional cardiac tissues.<sup>55,56</sup>

Because of a rough surface and adsorption of biomolecules like growth factors on the GR surface, it might provide possibilities to stimulate stem cells to differentiate into cardiomyocytes resulting in an improved contraction of the heart muscles. In addition, the conductive nature of GR can improve the organization and electrophysiological traits of the implanted stem cells. Moreover, because of its

anti-platelet adhesion and anticoagulant nature, GR can prevent blood clotting on the heart valve and can be used for the treatment of cardiovascular diseases. GR stimulates vasculogenesis and improves the viability of cells within a 3D environment mainly due to its electrophysiological and mechanical properties.<sup>24,25,57</sup>

Likewise, because of rGO electrical conductivity, it can control the proliferation, migration, and differentiation of cells in a tissue that requires proper electrical properties for cell-cell electrical interactions. An electrical extracellular microenvironment can be provided by an rGO-based 3D foam that can enable the electrical stimulation of cardiac cells with a uniform electric field strength distribution.<sup>52,58-60</sup>

Jing et al developed dopamine (DA)-loaded CS/GO composite hydrogels with enhanced conductivity in comparison with the CS-DA hydrogel. Via physical or chemical crosslinking, polydopamine (PDA) could react with CS to form a CS/GO composite hydrogel with enhanced mechanical stability. This structure was evaluated in terms of conductivity, self-healing, and adhesion of scaffold in cardiac and muscle tissue engineering (Fig. 1A). Due to electrical conductivity, rGO has been reported to provide a faster spontaneous beating rate in cardiomyocyte cells (Fig. 1B). Using live/dead assay, prepared hydrogels were also evaluated for their biocompatibility. The most viable results were obtained at a moderate concentration of GO in CS-DA-GO, whereas a high GO concentration led to more oxidative stress and more apoptotic cells (Fig. 1C). An adequate amount of GO has been shown to enhance cellular adhesion due to its strong affinity to ECM proteins. Moreover, the hydrogel was more crosslinked due to electrostatic interactions between CS and GO as well as PDA within the GO layers. The higher crosslinking density thereby resulted in a less swelling hydrogel with greater stability. It was shown that the electrical conductivity, self-healing, and adhesiveness of the CS/GO composite hydrogels could be enhanced in the presence of PDA, making it a potential candidate in electroactive tissue engineering.<sup>61</sup>

#### **Natural polymer and graphene hybrid scaffolds**

Shin et al recently reported the synthesis of rGO-loaded gelatin methacryloyl (GelMA) hybrid hydrogel for CTE that can be crosslinked using UV (Fig. 2A). Because of the strong non-covalent interaction between rGO and Gel methacryloyl (MA), no aggregation of rGO sheets was observed, potentially favoring the uniform distribution in the hydrogel matrix. The rGO sheets adsorb ECM proteins by  $\pi$ - $\pi$  stacking and hydrophobic interaction and induce greater cellular adhesion on the hybrid hydrogel. In comparison with pristine GelMA, and rGO, the rGO-GelMA hybrid hydrogel resulted in greater cell distribution, synchronous contraction, more cardiac markers, and much higher spontaneous beating rates due to the electrical and mechanical properties of

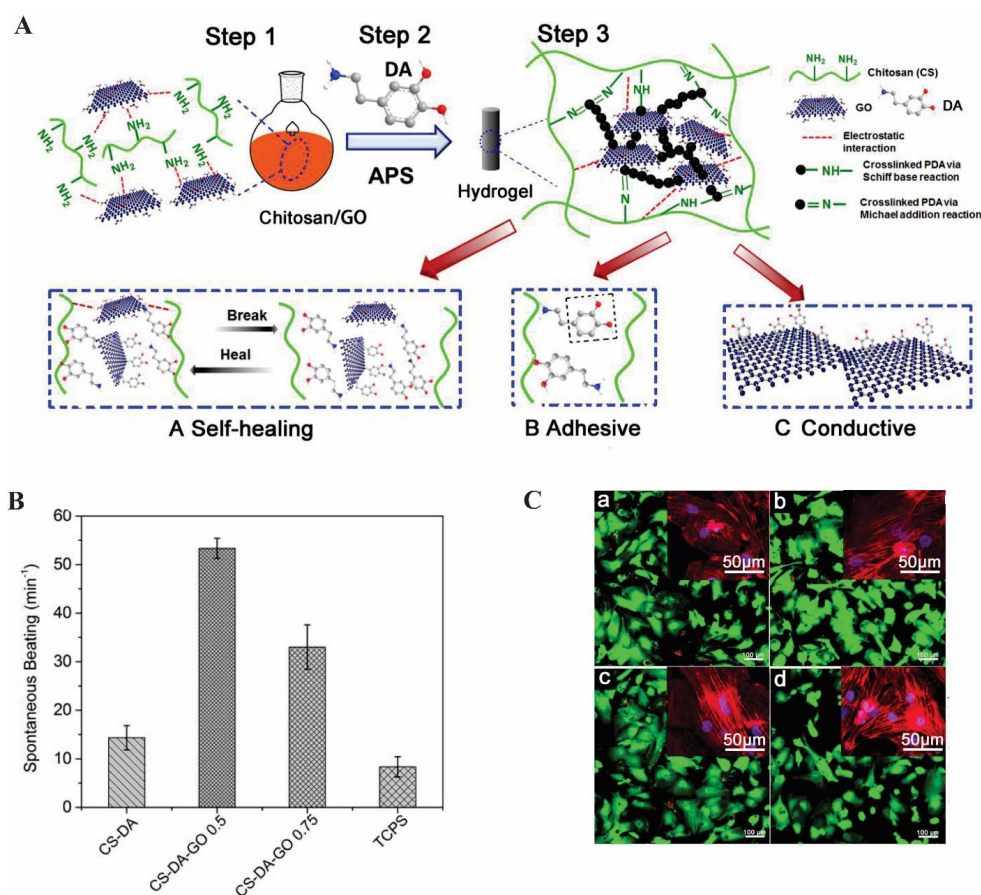


**Fig. 1.** The application of the CS-DA-GO scaffold in electroactive tissue engineering. (A) Schematic of CS-DA-GO composite hydrogel production. (B) Spontaneous beating rate of CMs on the selected hydrogels and TCPS. (C) Live/dead images of cells on (a) CS-DA, (b) CS-DA-GO 0.5, (c) CS-DA-GO 1, and (d) TCPS.<sup>61</sup> Copyright 2017. Reproduced with permission from Elsevier. CS-DA-GO, chitosan- dopamine- graphene oxide.

the hybrid hydrogel. The rGO's electrical and mechanical properties were measured by Young's modulus. The results showed that the rigidity and electrical conductivity of the hydrogel was enhanced when rGO was present in the hydrogel hybrid (Fig. 2B). Cardiac marker expressions were examined by cardiomyocyte immunostaining and the result showed a homogenous distribution, aligned and uniaxially structures of connexin 43 (Cx-43) and sarcomeric  $\alpha$ -actinin on rGO-GelMA hydrogel as compared to pristine GelMA samples. As a result, the rGO-GelMA hydrogel improved the beating behavior of the cardiac cells and contractile function (Fig. 2C). The SEM analysis also confirmed that less porous hydrogels were obtained at higher rGO concentrations. Moreover, based on live/dead assay and DNA concentration data, the 3T3 cells and primary cardiomyocytes cultured on the rGO-GelMA scaffolds exhibited more cytocompatibility, viability, and proliferation.<sup>62</sup> Overall, rGO incorporation into the biocompatible hydrogel appears to hold great promise for CTE to treat MI. The use of GO in CS-based composite scaffolds increased the electrical conductivity (0.134 S/m) in 150 mg/L GO/CS scaffold without exogenous electrical stimulation. Seven days after H9C2 was cultured in the GO/CS scaffold, the CX-43 and cTnT

genes, which are responsible for electrical coupling and muscle contraction, were up-regulated (4.1-fold) and down-regulated (1.3-fold), respectively.<sup>63</sup>

### Synthetic polymer and graphene hybrid scaffolds

To confirm the anisotropic electrical conductivity and structural organization of GR, Smith et al,<sup>64</sup> designed a micro-, and nano-patterned conductive GR-PEG hybrid scaffold to generate cardiac tissue constructs by grafting micro- and nano-patterned PEG onto the GR/poly(methyl methacrylic acid) (PMMA) layer. A float GR/PMMA in the groove region was first produced, and the PMMA was then removed by rinsing in isopropyl alcohol (Fig. 3A). The topography of the engineered GR-PEG structure was characterized by utilizing conductive atomic force microscopy (AFM), I-V curves and Raman spectroscopy. AFM analysis exhibited deposited GR film hung over the groove regions because of discrete crack formation and flat over the patterned ridges. The anisotropic electrical conductivity of GR-PEG was confirmed by I-V curves and the conductive AFM analysis. The I-V curves indicated the lowest resistance for GR-PEG in the parallel orientation of patterned ridges. Further, the highest resistance was recorded in transverse orientation, while the anisotropic

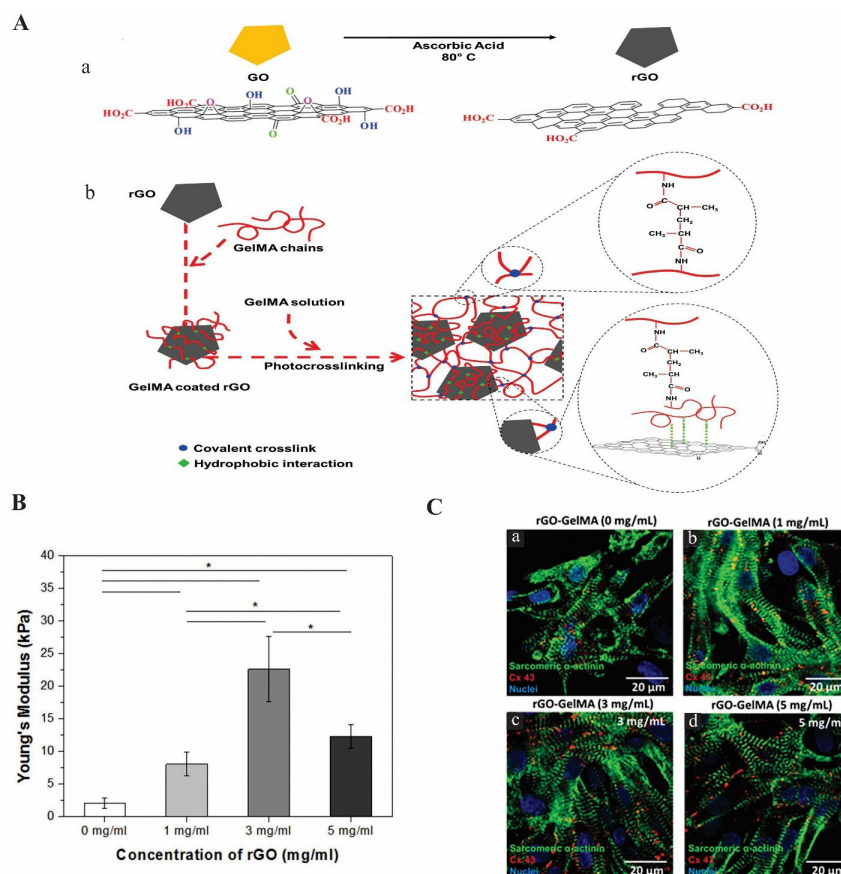


**Fig. 2.** The impact of rGO-GelMA hydrogel on cardiomyocytes in cardiac tissue engineering. (A) Illustration of the rGO-GelMA synthesis. (a) production of rGO from GO. (b) Preparation of rGO-GelMA hybrid hydrogels. (B) The elastic modulus of rGO-GelMA with rGO concentration. (C) Immunostaining of cardiomyocytes cultured on rGO-GelMA hydrogels for cardiac markers as a sarcomeric  $\alpha$ -actinin (green) and connexin 43 (red) after 8 days (a) 0 mg mL<sup>-1</sup>, (b) 1 mg mL<sup>-1</sup>, (c) 3 mg mL<sup>-1</sup>, (d) 5 mg mL<sup>-1</sup>.<sup>62</sup> Copyright 2016. Reproduced with permission from the Wiley Online Library. rGO-GelMA, reduced graphene oxide-gelatin methacryloyl.

electrical conductivity of the substrate was shown to be at the macroscopic scale. AFM analysis showed that GR-PEG conductivity was largely dependent on the orientation of the structure. The highest and the lowest electrical conductivity values were recorded respectively at the top surface of the patterned ridges and within the grooves. This is because cracks could cause anisotropic electrical conductivity patterns at the microscale. The addition of oxygen plasma to the GR-PEG substrate also increased the anisotropic electrical conductivity on the ridges of the oxygen plasma-treated substrate due to the removal of residual PMMA polymer. On the contrary, longer plasma exposure increased GR defects within the groove regions and reduced conductivity. To evaluate the suitability of GR-PEG substrate for cardiac tissue engineering, the effect of anisotropic electroconductive and topographic cues on cardiac cell function and structure was considered. Contractile and beating pulse behaviors or structural properties of cardiac cells on oxygen plasma-treated GR-PEG (OGR-PEG) substrate were known by immunostaining with antibodies against  $\alpha$ -actinin, a sarcomeric protein localized to the Z disc and Cx43. All three scaffolds of PEG, GR-PEG-G, and OGR-PEG showed highly organized actin-myosin contractile

units and circumferential distribution of Cx43 on cardiac cells. Confocal microscopy analysis revealed that cardiac cells grown on PEG-OG scaffolds displayed larger average sarcomere length– key for correlating inversely with a cell’s ability in terms of generating contractile force and larger z-band widths – as compared to cardiac cells grown on PEG scaffolds. Western blotting was used to measure glyceraldehyde-3-phosphate dehydrogenase (GAPDH) expression in response to an electrophysiological function of the heart by changing Cx43 and SERCA2, and the results showed that the levels of SERCA2 and Cx43 expression in cardiac cells grown on OGR-PEG were higher than other scaffolds (Fig. 3B). Hydrophilicity and binding of cells to the scaffold were enhanced by treating GR-PEG with oxygen-plasma which led to improving cell attachment, growth, and maturation. Because of enhancement in Ca<sup>2+</sup> transient<sup>65</sup> and the upregulation of SERCA2 protein expression, calcium release during depolarization events was enhanced when cardiac cells were cultured on OGR-PEG surfaces (Fig. 3C). Therefore, PEG functionalized GR with an anisotropic electrical conductivity appears to improve the cell-cell coupling, modulate calcium handling proteins, regulate the electrophysiological function of the heart, and enhance myofibrils and

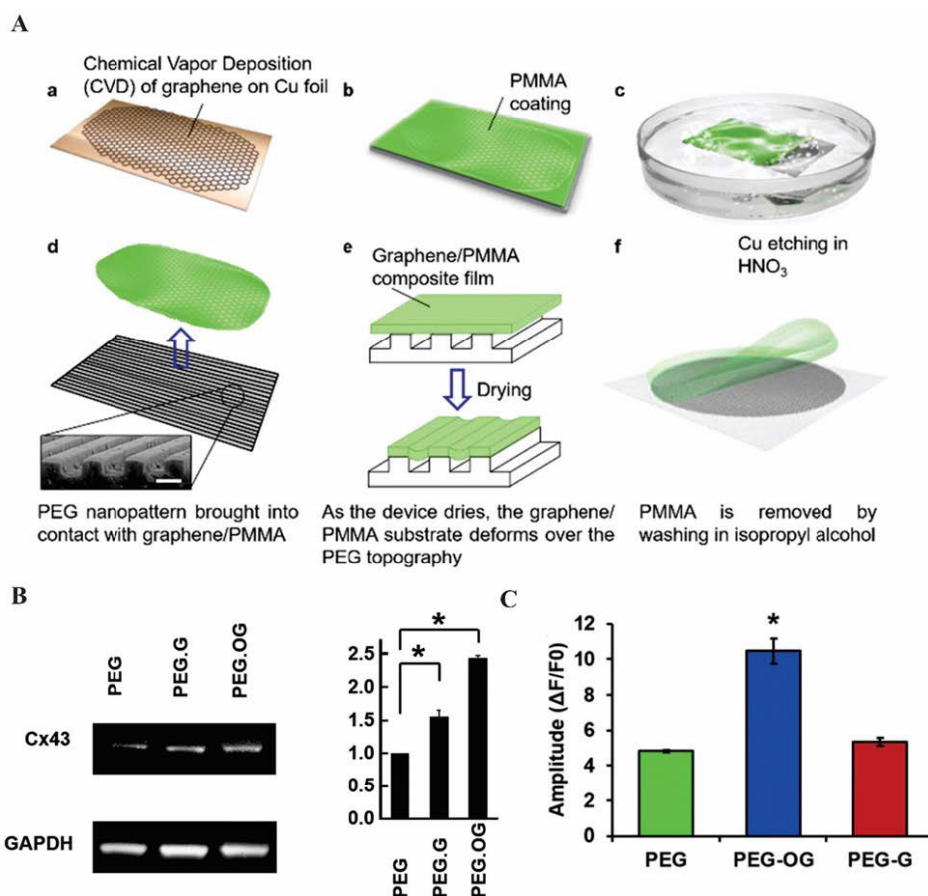


**Fig. 3.** The micro- and nano-patterned conductive GR-PEG hybrid scaffold for cardiac tissue engineering. (A) Illustration of patterned conductive GR-PEG hybrid scaffolds process. (a) A GR layer formation by chemical vapor deposition (CVD) on copper foil, (b) PMMA coated on GR layer, (c) The copper foil was etched in an HNO<sub>3</sub> bath, (d) GR/PMMA composite was placed in water and PEG patterns were raised to contact with the topography, (e) The GR/PMMA was dried on PEG substrate. GR/PMMA in the groove region was prepared by the GR/PMMA layer wets the micro- and nano-patterned PEG, (f) G-PEG was washed with isopropyl alcohol and rinsed in de-ionized water. (B) Characterization of gap junction protein expression by Western blot analysis and Quantification of Cx43 expression in PEG, PEG.G, and PEG.OG. (C) Analysis of calcium transient waveforms and Ca<sup>2+</sup> transient amplitude of PEG, PEG.G, PEG.OG in the grown cardiac cells.<sup>64</sup> Copyright 2017. Reproduced with permission from the Royal Society of Chemistry. GR, graphene; PMMA, poly(methyl methacrylate); PEG, polyethylene glycol.

sarcomeres contraction with calcium release ability. Thus, it may be considered an exciting substrate for advanced CTE.<sup>64</sup> rGO-silver nanocomposites incorporated into PU nanofibrous scaffold (rGO-Ag-PU) were fabricated via the electrospinning method. The Ag nanoparticles (NPs) enhanced the electrical conductivity of rGO while the rGO restricted the aggregation of AgNPs. The mechanical strength, electrical conductivity, and wettability of the PU scaffold were improved in the presence of rGO-Ag. The upregulation of cardiac-specific genes encompassing T-box 18 (TBX 18), GATA-4, cTnT, and alpha-myosin heavy chain (α-MHC) and more hCPCs proliferation (Fig. 4A, B) was observed for PU/rGO-Ag (1 and 2 wt%) scaffolds. Immunofluorescent staining of α-Actinin and cTnT confirmed more upregulation of cardiac-specific genes in the PU/rGO-Ag scaffolds (Fig. 4C).<sup>66</sup> In addition, echocardiography (ECHO) of injectable oligo(polyethylene glycol fumarate) (OPF)/GO(OPF/GO) hydrogel revealed the improvement of ejection fraction and fractional shortening after 4 weeks of injection in the myocardial infarcted region. The addition of GO into

OPF hydrogels promoted the alpha-smooth muscle actin (α-SMA), vWF, and VEGF, suggesting the angiogenesis effect of OPF/GO hydrogel. By bridging the OPF, GO seems to modulate the pathways for transmitting electric flow and rhythmic calcium transients.<sup>67</sup>

### Peptide and protein-functionalized graphene hybrid system

A new multilayer cell construct of poly-L-lysine (PLL) coated GO sheets and alternative cell seeding with interlayer connectivity were prepared by a systematic layer-by-layer assembly technique (Fig. 5A, B). Cells cultured on the carbon nanotube (CNT)-GelMA and pristine GelMA hydrogel substrates were used to assess the appropriateness of hybrid hydrogels as the primary substrates. The results showed that the cells seeded on the GO-GelMA substrates were larger, more homogenous, and more elongated than other substrates, and also showed similar compressive modulus to CNT-GelMA gels. Therefore, the GO-GelMA substrate was used as the main scaffold to prepare multilayered constructs. Due to

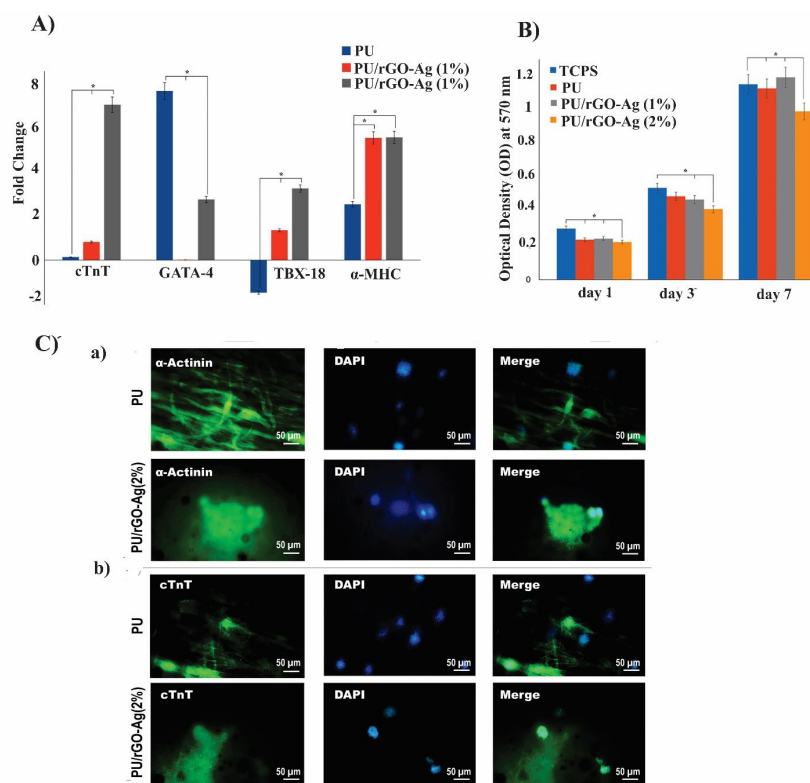


**Fig. 4.** The biological effect of the rGO-Ag-PU nanofibrous scaffold on hCPCs for cardiac tissue engineering. (A) The levels of cardiogenic gene expression of hCPCs on PU, PU/rGO-Ag (1%), and PU/rGO-Ag (2%) scaffolds. (B) MTT assay using optical densities. (C) Immunofluorescent staining of hCPCs on PU, PU/rGO-Ag (1%), and PU/rGO-Ag (2%) scaffolds.<sup>66</sup> Copyright 2019. Reproduced with permission from Wiley Online Library. Ag, silver; PU, polyurethane; hCPCs, human cardiac progenitor cells.

the electrostatic attraction between the negatively charged GO surfaces and positively-charged PLL chains, PLL in the GO-PLL could act as an adhesive between each cell layer, building strong cell adhesion, enhancing cell-cell interaction and biological activity. The architecture and thickness of multilayer tissue were controlled by adjusting the quantity of the deposited GO. More homogenous deposited PLL-GO was observed when a higher concentration of PLL-GO was used. The fabrication of multilayer cardiac tissues was further investigated according to the layer-by-layer (LbL) assembly technique of culturing cardiomyocytes, endothelial cells, and human mesenchymal stem cells (hMSCs) on the GO/PLL films. In this strategy, cardiac-specific marker sarcomeric  $\alpha$ -actinin, contraction function, and beating behavior under a low external electric field were enhanced due to the presence of PLL-GO film that promoted cardiomyocyte maturation, guided cell-cell interaction by organized cell networks, and induced cell-cell electrical coupling. This can mainly be attributed to the impedance reduction that might accelerate the charge distribution between cells. Their findings indicated that the three cell types co-cultured on GO/PLL films showed great applicability in terms of 3D cultivation of cardiac tissue with a high level of cell viability and adhesion along with electrophysiological function and programmable pumping properties.<sup>68</sup> Electroactive composite Col-GO and Col-rGO scaffolds have shown

potential for assisting vascularization and cardiac tissue engineering. The Col-GO scaffold was fabricated by covalent binding between  $-NH_2$  groups of the Col and  $-COOH$  groups of GO, which indicated randomly oriented interconnected pores in the desirable range of  $120-138 \pm 8 \mu m$ . The tensile strength and Young's modulus of Col-GO-90 were enhanced to 162 kPa and 750 kPa, respectively. In addition, Col-rGO scaffold was shown to promote the neonatal CM adhesion, proliferation, and upregulation of troponin T type 2 (TrpT-2), Cx43, and actinin alpha 4 (Actn4) as cardiac gene markers. Because of the angiogenesis properties of rGO, more blood vessels and capillaries formed within the Col-rGO-90 scaffolds as confirmed by immunofluorescent staining.<sup>69</sup>

### Cardiomyogenic differentiation on graphene hybrid material

It has been recently reported that GR is required to stimulate the cardiomyogenic differentiation of human embryonic stem cells (hESCs). The concept was confirmed by GR-coated vitronectin (GR-VN) used for high cell viability and a substantial degree of cardiomyogenic differentiation. Owing to the rough nanoscale structure of GR, it seems to induce hESC adhesion, promoting the expressions of cardiomyogenic genes such as cardiac-specific ECM, extracellular signal-regulated kinase (ERK), and focal adhesion kinase (FAK) signaling. As a





and biodegradation within the cells (Fig. 6B).

Interestingly, stem cell proliferation decreased in EB-GR as compared to EB, presumably because GR limited the cell-cell compression and increased cell differentiation. Given its electrical conductivity at a concentration of 0.2 mg mL<sup>-1</sup>, GR can effectively differentiate the stem cells in EB-GR. Moreover, because of its high mechanical strength, GR enhanced Young's modulus of EBs and affected stem cell differentiation into different lineages. According to high-throughput gene analysis, the differentiation of stem cells in EB-GR significantly increased as compared to EB on day 5 of culture due to the electrical and mechanical properties of GR. The effect of electrical stimulation on the cardiomyogenesis of stem cells was evaluated by the cardiac protein levels, expression of cardiac genes, and beating activity of the EBs and EB-GR. Upon electrical stimulation, the TrpT-2 expression of EB-GR was found higher than EB due to GR's natural electrical conductivity. The data showed an enhanced TrpT-2 level for EB-GR and EB as compared to the control with no electrical stimulation. The EB immunostaining of cell nuclei and TrpT-2 led to similar results (Fig. 6C). Moreover, cardiac gene expression (e.g., Actc1, Myh6, Myh7, and Tnnt2) induced by EB-GR upon electrical stimulation was found to be greater than that of the EB in the absence of electrical stimulation. Based on the beating activity, the number of beats per minute, the average displacements of

EB-GR, and the ratio of the EB beating area to the whole EB area for EB-GR with electrical stimulation were found greater than EBs and EB-GR in the absence of electrical stimulation. These data support the fact that EB-GR can potentially be used as a platform for cardiac differentiation and stem cell culture for regenerative applications.<sup>80</sup> In one study, 3D graphene foam (3D-GF) and two-dimensional GR (2DG) were prepared by CVD. The morphological analyses of the porous 3D-GFs showed that the structure was fully interconnected and 95% of the pores were 100–300 nm in size. Fluorescence-staining images showed that human umbilical vein endothelial cells (HUVECs) cultured on a 3D-GF scaffold were more integrated due to the appropriate 3D environment for cardiac cells. The 3D-GF electrical conductivity of 9 S/cm<sup>-1</sup> was desirable for neuronal differentiation, proliferation, and myocardial tissue applications. The 3D-GF provided higher levels of Conx43 and TrpT-2 genes as compared to 2DG and TCP due to acceptable electroactive moieties for cardiomyogenic stimulation.<sup>81</sup> Table 1 lists some important aspects of GR-based materials in CTE and regeneration.

### Biocompatibility of graphene-polymer materials

Before using GR-based materials for biomedical purposes, it is important to analyze their toxicity and biocompatibility *in vivo* and *in vitro*. Due to the jagged edge, GR has been shown to damage the lung

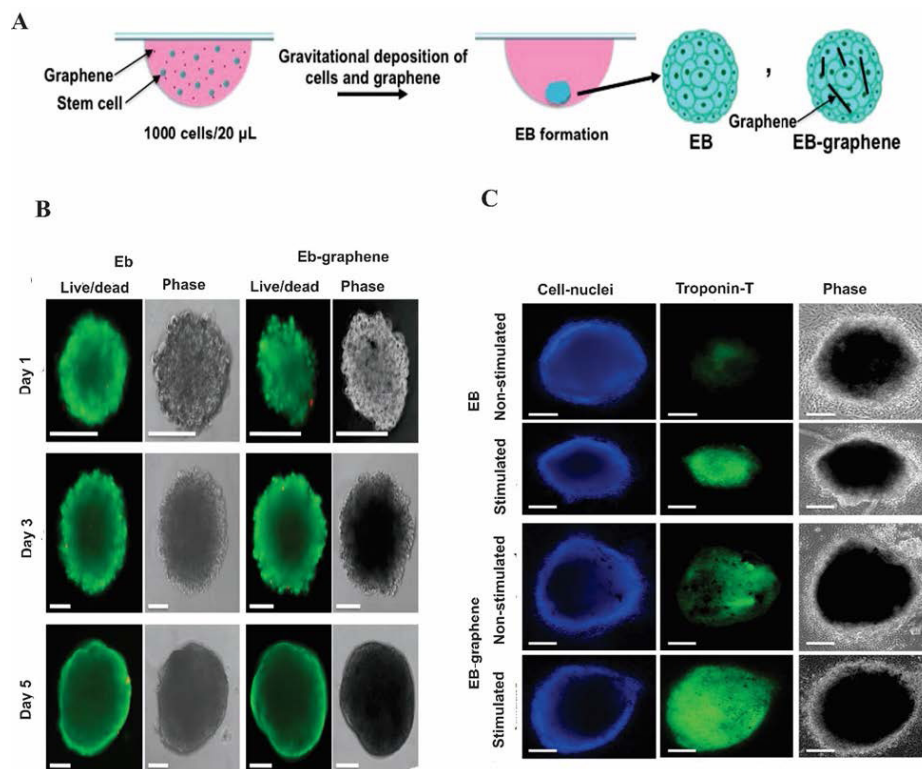


**Fig. 6.** The effect of the EB-GR platform in cardiac regeneration. (A) Illustration of the EB formation using the hanging drop technique. (B) Images of live and dead mouse embryonic stem cells on EBs and the EBs containing 0.2 mg per mL GR at different times. (C) Immunostaining of cell nuclei and TrpT-2 with and without electrical stimulation.<sup>80</sup> Copyright 2016. Reproduced with permission from the Royal Society of Chemistry. EB, embryoid bodies; TrpT-2, Troponin T type 2.

**Table 1.** Application of the graphene-based material in cardiac tissue engineering and regeneration

Graphene type	Polymers	Cell line	Methods	Analysis applied	Outcomes or cell behavior	Applications	Ref.
rGO	Gelatin methacryloyl (GelMA)	3T3 cells and primary cardiomyocytes	rGO-GelMA hybrid hydrogel	TEM, AFM, Elastic modulus, Electrical impedance, Immunostaining, Electrophysiological measurement, Cellular DNA concentration, Live/dead assay	Homogeneous cell distribution, Synchronous contraction, Increased spontaneous beating rates, more cardiac markers, Enhanced electrical conductivity, and mechanical rigidity, Cytocompatibility, Cell proliferation	Cardiac tissue engineering	62
GO	PLL/ GelMA	Cardiomyocytes, Endothelial cells and hMSCs, 3T3 fibroblast cells, ECs	Layer-by-layer assembly technique	Fluorescence images, SEM, Hematoxylin and Eosin (H&E) stain, MTS, Live/dead assay	Mechanical integrity, High organization, Cell maturation, Cell adhesion, Viability, Enhanced contraction function, Strong beating behavior	Cardiac tissue engineering	68
GR	PEG	Cardiac cell	Covering PEG micro- and nano-patterned into GR/PMMA layer	AFM, Conductive AFM, I-V curves, Western blot analysis, Immunostaining, Analysis of calcium transient waveforms	Cell attachment, growth, and maturation, Increased hydrophilicity, Sarcomeres contraction, High expression of SERCA2 and Cx43	Cardiac tissue engineering	64
GR	Vitronectin (VN)	Human embryonic stem cells (hESCs)	GR coating with VN	Contact angle, TEM, Western blot analyses, qRT-PCR	Upregulation of ERK, FAK, vinculin, and paxillin, Not filled contractile cardiomyocytes differentiation	Cardiomyogenic differentiation	70
GR	-	MSCs	CVD	AFM, TEM, qRT-PCR, Live/dead assay, Apoptotic cell, Proliferation test by PCNA staining, and hemocytometer	Increased contractile proteins and gap junction protein expression, Upregulation of FAK and PI3K/Akt, Cell Proliferation, Differentiation, viability	Cardiomyogenic differentiation	82
GR	-	129/SVE-derived mouse stem cells	GR-EB (embryoid bodies) by the hanging drop technique	Live /dead cells, Current-voltage measurements, Mechanical measurement, High-throughput gene analysis, Immunostaining, qRT-PCR, Beating analysis	High mechanical strength and Young's modulus, Biocompatibility, Decreased cell proliferation, Increased cardiac genes and protein expression in the presence of electrical stimulation, Beating behavior	Cardiomyogenic differentiation	80

cell membrane through penetration and induced cell apoptosis and toxicity.<sup>83</sup> It has been shown that GR can induce ROS generation and depolarization of mitochondrial membranes in HUVECs.<sup>84</sup> The ROS generated this way can cause excessive DNA damage and increase the numbers of monocytes and proinflammatory cytokines, resulting in an inflammatory environment.<sup>85</sup> The toxicity and biocompatibility of GR-based material are largely dependent on physicochemical properties (e.g., shape, size, surface charge, and concentration), the composition of GR-based material (surface modification and its hydrophilicity), and the amount of formed ROS. Given the correlation of toxicity with shape and surface modification, the toxicity of rGO and carboxylated GR has been reported to be less than GO or pure GR in the monkey kidney cells.<sup>86</sup> GO also showed less toxicity than GR.<sup>86</sup> Moreover, larger lateral dimensions of rGO induced less cytotoxicity as compared to smaller lateral dimensions due to the entrance of small particles to human MSC cells via endocytosis<sup>87</sup> and the uptake of large fragments through phagocytosis.<sup>88</sup> In addition, given the effect of GO concentration, minimum cell toxicity was observed in A549 cells when 50 µg/mL of GO sheet was used, and toxicity was increased at higher GO concentrations.<sup>89</sup> *In vivo* toxicity of GR was shown to be due to accumulation in the lung, long blood circulation time, and low uptake or capture into the reticuloendothelial system as compared to nontoxic materials. A 14-day biocompatibility study showed that GO offers good biocompatibility with red blood cells at 1 mg kg<sup>-1</sup> body weight, whereas toxicity and inflammatory response were apparent when GO was used 10 times as much.<sup>90</sup>

The functionalization of nanographene sheets (NGSs) with PEG was found to increase the hydrophilicity of GR and reduce *in vivo* toxicity. Of note, the PEGylated NGS mostly gathered in the reticuloendothelial system, including the spleen and liver (similar to most nanomaterial), and could be gradually cleared over 3 months.<sup>91,92</sup> Ming et al investigated the toxicity of functionalized GO with poly(acrylic acid) (PAA), polyacrylamide (PAM), PEG, and aminated groups. Among these GO derivatives, GO-PAA showed the best biocompatibility *in vitro* and *in vivo* and less toxicity on J774A.1 cell. Since GO-PEG and GO-PAA posed fewer protein coronas absorption, the secondary structure of IgG was less affected, resulting in less interaction with cell membrane proteins. Thus, less membrane disruption and less endocytosis with improved viability were indicated.<sup>93</sup>

It has been well documented that the covalent functionalization of GO with dextran (DEX) as a biocompatible polymer (GO-DEX), with 50–100 nm size and 2.8 nm width reduced HeLa cell toxicity and improved its biocompatibility. GO-DEX accumulated in RES after injection and it was excreted via both renal and fecal routes from the mouse body within a week without noticeable toxicity.<sup>94</sup> Chowdhury et al reported

on *in vitro* and *in vivo* nontoxicity of O-GNR-PEG-DSPE up to 80 µg/mL concentration of GO in endothelial cells (HUVEC cells) due to functionalization of GR nanoribbons with PEG-DSPE (1, 2-distearoyl-*sn*-glycerol-3-phosphoethanolamine-*N* [amino (polyethylene glycol)]) as a hematological component in treating of circulatory system diseases.<sup>95</sup> In another study, the hydroxypropyl CS-graft-GO (HPCH-g-GO) 3D scaffold was prepared by the freeze-drying technique and showed more uniform porosity and interconnectivity compared to the HPCH scaffold. Swelling capacity, water retention ability, and mechanical strength were improved when 1% GO was added. *In vitro*, biocompatibility confirmed good cell viability with no obvious cytotoxicity of the HPCH-g-GO scaffold against mouse C3H10T1/2 MSCs as compared to the control group. As a result, the HPCH-g-GO scaffold was proposed as a potential platform for tissue engineering.<sup>96</sup> Overall, although GR can be a promising material in tissue engineering and biomedical applications, more efforts need to be made to understand the *in vivo* long-term biodistribution and cytotoxicity of GR-based material before they can practically be used in the clinical setting.

#### Final remarks

Tissue engineering has paved the way for a longer life expectancy. Accordingly, various advanced materials have been used for the development of 3D scaffolds. To date, much attention has been paid to the use of GR-incorporated biomaterials in tissue engineering and regenerative medicine mainly due to their extraordinary mechanical, electrical, and biological properties. GR-modified biomaterials have been shown to provide a permissive setting to the embedded stem cells and improve their proliferation and differentiation in favor of myocardial tissue. GR and its derivative, because of free  $\pi$  electron and negative charges, have also been used as a gene/drug delivery system, indicating their potential for delivery of drugs to the targeted cells/tissues. GR and its derivative have been used to improve the mechanical and surface properties of materials to direct stem cell differentiation into different types of cells (e.g., chondrocytes and cardiomyocytes), and to inhibit the thrombosis on artificial heart valves. A series of studies focused on cell proliferation and adhesion using GR-based materials (for the regeneration of cardiac, and vascular tissues) have proven their impacts in tissue engineering. Further, due to its electrical properties, GR can be used for the development of various tissues (e.g., cardiovascular tissues) that needs conductivity for the generation of electrical impulses/signals. To date, a myriad of literature has shown that GR might be used in biomedical applications even though somewhat cytotoxic and/or genotoxic effects may limit its applications. Such a potentially hazardous aspect of GR can be resolved via surface modifications. That being emphasized, the

## Review Highlights

**What is the current knowledge?**

- ✓ Cardiac tissue engineering has been advanced using safe natural or synthetic scaffolds with preferred substances.
- ✓ Graphene is a two-dimensional form of crystalline carbon, which can become an appreciated and useful nanomaterial because of its remarkably high tensile strength and electrical conductivity.
- ✓ Graphene can be modified with different polymers becoming a potential scaffold for cardiac tissue engineering.

**What is new here?**

- ✓ Graphene-modified biomaterials can provide a potential setting for the laden stem cells and recover their growth and differentiation in the approval of myocardial organs.
- ✓ Graphene can be utilized for the improvement of numerous tissues such as cardiovascular organs that requires conductivity for the production of electrical impulses/signals.
- ✓ Graphene and its derivative have been utilized to increase the mechanical and surface belongings of platforms to provide stem cell differentiation into different kinds of cells such as cardiomyocytes.

long-term in vivo safety of standardized GR products necessitates a systematic investigation.

**Acknowledgments**

The authors acknowledge the support from the Research Center for Pharmaceutical Nanotechnology at Tabriz University of Medical Sciences.

**Authors' contribution**

**Conceptualization:** Marziyeh Fathi & Nazanin Amiryaghoubi.

**Investigation:** Marziyeh Fathi & Nazanin Amiryaghoubi.

**Supervision:** Marziyeh Fathi.

**Writing—original draft:** Nazanin Amiryaghoubi.

**Writing—review & editing:** Marziyeh Fathi & Nazanin Amiryaghoubi.

**Competing Interests**

None to be declared.

**Ethical Statement**

Not applicable.

**References**

1. Conn PM. *Animal models for the study of human disease*. Academic Press; 2017.
2. Rodrigues ICP, Kaasi A, Maciel R, Jardim AL, Gabriel LP. Cardiac tissue engineering: current state-of-the-art materials, cells and tissue formation. *Einstein (Sao Paulo)* 2018; 16: eRB4538. <https://doi.org/10.1590/S1679-45082018RB4538>
3. Camci-Unal G, Annabi N, Dokmeci MR, Liao R, Khademhosseini A. Hydrogels for cardiac tissue engineering. *NPG Asia Mater* 2014; 6: e99-e. <https://doi.org/10.1038/am.2014.19>
4. Ahmadi P, Nazeri N, Derakhshan MA, Ghanbari H. Preparation and characterization of polyurethane/chitosan/CNT nanofibrous scaffold for cardiac tissue engineering. *Int J Biol Macromol* 2021; 180: 590-8. <https://doi.org/10.1016/j.ijbiomac.2021.03.001>
5. Villalobos Lizardi JC, Baranger J, Nguyen MB, Asnacios A, Malik A, Lumens J, et al. A guide for assessment of myocardial stiffness in health and disease. *Cardiovasc Res* 2022; 1: 8-22. <https://doi.org/10.1038/s44161-021-00007-3>
6. Amiryaghoubi N, Fathi M, Pesyan NN, Samiei M, Barar J, Omidi Y. Bioactive polymeric scaffolds for osteogenic repair and bone regenerative medicine. *Med Res Rev* 2020; 40: 1833-70. <https://doi.org/10.1002/med.21672>
7. Geim AK. Graphene: status and prospects. *science* 2009; 324: 1530-4. <https://doi.org/10.1126/science.1158877>
8. Chaudhuri B, Bhadra D, Mondal B, Pramanik K. Biocompatibility of electrospun graphene oxide-poly ( $\epsilon$ -caprolactone) fibrous scaffolds with human cord blood mesenchymal stem cells derived skeletal myoblast. *Mater Lett* 2014; 126: 109-12. <https://doi.org/10.1016/j.matlet.2014.04.008>
9. Stevanović M, Djošić M, Janković A, Kojić V, Vukašinić-Sekulić M, Stojanović J, et al. Antibacterial Graphene-Based Hydroxyapatite/Chitosan Coating with Gentamicin for Potential Applications in Bone Tissue Engineering. *J Biomed Mater Res A* 2020; 108: 2175-89. <https://doi.org/10.1002/jbm.a.36974>
10. Khalili R, Zarrintaj P, Jafari SH, Vahabi H, Saeb MR. Electroactive poly (p-phenylene sulfide)/r-Graphene Oxide/Chitosan as a novel potential candidate for tissue engineering. *Int J Biol Macromol* 2020; 154: 18-24. <https://doi.org/10.1016/j.ijbiomac.2020.03.029>
11. Schöche S, Hong N, Khorasaninejad M, Ambrosio A, Orabona E, Maddalena P, et al. Optical properties of graphene oxide and reduced graphene oxide determined by spectroscopic ellipsometry. *Appl Surf Sci* 2017; 421: 778-82. <https://doi.org/10.1016/j.apsusc.2017.01.035>
12. Amiryaghoubi N, Fathi M, Barar J, Noroozi-Pesyan N, Omidian H, Omidi Y. Application of graphene in articular cartilage tissue engineering and chondrogenic differentiation. *J Drug Deliv Sci Technol* 2023; 83: 104437. <https://doi.org/10.1016/j.jddst.2023.104437>
13. Amiryaghoubi N, Fathi M, Barzegari A, Barar J, Omidian H, Omidi Y. Recent advances in polymeric scaffolds containing carbon nanotube and graphene oxide for cartilage and bone regeneration. *Mater Today Commun* 2021; 26: 102097. <https://doi.org/10.1016/j.mtcomm.2021.102097>
14. Wang C-H, Guo Z-S, Pang F, Zhang L-Y, Yan M, Yan J-H, et al. Effects of graphene modification on the bioactivation of polyethylene-terephthalate-based artificial ligaments. *ACS Appl Mater Interfaces* 2015; 7: 15263-76. <https://doi.org/10.1021/acsami.5b02893>
15. Amiryaghoubi N, Fathi M, Barar J, Omidian H, Omidi Y. Recent advances in graphene-based polymer composite scaffolds for bone/cartilage tissue engineering. *J Drug Deliv Sci Technol* 2022; 72: 103360. <https://doi.org/10.1016/j.jddst.2022.103360>
16. Amiryaghoubi N, Fathi M, Barar J, Omidian H, Omidi Y. Hybrid polymer-grafted graphene scaffolds for microvascular tissue engineering and regeneration. *Eur Polym J* 2023; 193: 112095. <https://doi.org/10.1016/j.eurpolymj.2023.112095>
17. Pinto AR, Ilinykh A, Ivey MJ, Kuwabara JT, D'antoni ML, Debuque R, et al. Revisiting cardiac cellular composition. *Circ Res* 2016; 118: 400-9. <https://doi.org/10.1161/CIRCRESAHA.115.307778>
18. Zhang YS, Aleman J, Arneri A, Bersini S, Piraino F, Shin SR, et al. From cardiac tissue engineering to heart-on-a-chip: beating challenges. *Biomed Mater* 2015; 10: 034006. <https://doi.org/10.1088/1748-6041/10/3/034006>
19. Tandon V, Zhang B, Radisic M, Murthy SK. Generation of tissue constructs for cardiovascular regenerative medicine: from cell procurement to scaffold design. *Biotechnol Adv* 2013; 31: 722-35. <https://doi.org/10.1016/j.biotechadv.2012.08.006>
20. Brown RD, Ambler SK, Mitchell MD, Long CS. The cardiac fibroblast: therapeutic target in myocardial remodeling and failure. *Annu Rev Pharmacol Toxicol* 2005; 45: 657-87.
21. You J-O, Rafat M, Ye GJ, Auguste DT. Nanoengineering the heart: conductive scaffolds enhance connexin 43 expression. *Nano Lett* 2011; 11: 3643-8. <https://doi.org/10.1021/nl201514a>

22. Dvir T, Timko BP, Brigham MD, Naik SR, Karajanagi SS, Levy O, et al. Nanowired three-dimensional cardiac patches. *Nat Nanotechnol* **2011**; 6: 720. <https://doi.org/10.1038/nnano.2011.160>
23. Kim HN, Jiao A, Hwang NS, Kim MS, Kim D-H, Suh K-Y. Nanotopography-guided tissue engineering and regenerative medicine. *Adv Drug Deliv Rev* **2013**; 65: 536-58. <https://doi.org/10.1016/j.addr.2012.07.014>
24. Gálvez-Montón C, Prat-Vidal C, Roura S, Soler-Botija C, Bayes-Genis A. Cardiac tissue engineering and the bioartificial heart. *Rev Esp Cardiol (Engl Ed)* **2013**; 66: 391-9. <https://doi.org/10.1016/j.rec.2012.11.012>
25. Radhakrishnan J, Krishnan UM, Sethuraman S. Hydrogel based injectable scaffolds for cardiac tissue regeneration. *Biotechnol Adv* **2014**; 32: 449-61. <https://doi.org/10.1016/j.biotechadv.2013.12.010>
26. Rushton C, Kadam U. Impact of non-cardiovascular disease comorbidity on cardiovascular disease symptom severity: a population-based study. *Int J Cardiol* **2014**; 175: 154-61. <https://doi.org/10.1016/j.ijcard.2014.05.001>
27. Ong K-L, Ding J, McClelland RL, Cheung BM, Criqui MH, Barter PJ, et al. Relationship of pericardial fat with biomarkers of inflammation and hemostasis, and cardiovascular disease: the Multi-Ethnic Study of Atherosclerosis. *Atherosclerosis* **2015**; 239: 386-92. <https://doi.org/10.1016/j.atherosclerosis.2015.01.033>
28. Sergi G, Veronese N, Fontana L, De Rui M, Bolzetta F, Zambon S, et al. Pre-frailty and risk of cardiovascular disease in elderly men and women: the Pro. VA study. *J Am Coll Cardiol* **2015**; 65: 976-83.
29. Ashtari K, Nazari H, Ko H, Tebon P, Akhshik M, Akbari M, et al. Electrically conductive nanomaterials for cardiac tissue engineering. *Adv Drug Deliv Rev* **2019**; 144: 162-79. <https://doi.org/10.1016/j.addr.2019.06.001>
30. Liu T, Sun F, Cui J, Zheng S, Li Z, Guo D, et al. Morroniside enhances angiogenesis and improves cardiac function following acute myocardial infarction in rats. *Eur J Pharmacol* **2020**; 872: 172954. <https://doi.org/10.1016/j.ejphar.2020.172954>
31. Lozano R, Naghavi M, Foreman K, Lim S, Shibuya K, Aboyans V, et al. Global and regional mortality from 235 causes of death for 20 age groups in 1990 and 2010: a systematic analysis for the Global Burden of Disease Study 2010. *The Lancet* **2012**; 380: 2095-128. [https://doi.org/10.1016/S0140-6736\(12\)61728-0](https://doi.org/10.1016/S0140-6736(12)61728-0)
32. MEMBERS WG, Benjamin EJ, Blaha MJ, Chiuve SE, Cushman M, Das SR, et al. Heart disease and stroke statistics—2017 update: a report from the American Heart Association. *Circulation* **2017**; 135: e146. <https://doi.org/10.1161/CIR.0000000000000485>
33. Nian M, Lee P, Khaper N, Liu P. Inflammatory cytokines and postmyocardial infarction remodeling. *Circ Res* **2004**; 94: 1543-53. <https://doi.org/10.1161/01.RES.0000130526.20854.fa>
34. Boateng SY, Lateef SS, Mosley W, Hartman TJ, Hanley L, Russell B. RGD and YIGSR synthetic peptides facilitate cellular adhesion identical to that of laminin and fibronectin but alter the physiology of neonatal cardiac myocytes. *Am J Physiol Cell Physiol* **2005**; 288: C30-C8. <https://doi.org/10.1152/ajpcell.00199.2004>
35. Hookway TA, Matthys OB, Mendoza-Camacho FN, Rains S, Sepulveda JE, Joy DA, et al. Phenotypic variation between stromal cells differentially impacts engineered cardiac tissue function. *Tissue Eng Part A* **2019**; 25: 773-85. <https://doi.org/10.1089/ten.tea.2018.0362>
36. Tao ZW, Mohamed M, Hogan M, Gutierrez L, Birla RK. Optimizing a spontaneously contracting heart tissue patch with rat neonatal cardiac cells on fibrin gel. *J Tissue Eng Regen Med* **2017**; 11: 153-63. <https://doi.org/10.1002/term.1895>
37. Feiner R, Shapira A, Dvir T. Scaffolds for tissue engineering of functional cardiac muscle. *Handbook of Tissue Engineering Scaffolds*; Elsevier; **2019**. p. 685-703.
38. Engler AJ, Carag-Krieger C, Johnson CP, Raab M, Tang H-Y, Speicher DW, et al. Embryonic cardiomyocytes beat best on a matrix with heart-like elasticity: scar-like rigidity inhibits beating. *J Cell Sci* **2008**; 121: 3794-802. <https://doi.org/10.1242/jcs.029678>
39. Hollister SJ. Porous scaffold design for tissue engineering. *Nat Mater* **2005**; 4: 518. <https://doi.org/10.1038/nmat1421>
40. Shi M, Bai L, Xu M, Li Z, Hu T, Hu J, et al. Micropatterned conductive elastomer patch based on poly (glycerol sebacate)-graphene for cardiac tissue repair. *Biofabrication* **2022**; 14: 035001. <https://doi.org/10.1088/1758-5090/ac59f2>
41. Duan B, Hockaday LA, Kang KH, Butcher JT. 3D bioprinting of heterogeneous aortic valve conduits with alginate/gelatin hydrogels. *J Biomed Mater Res A* **2013**; 101: 1255-64. <https://doi.org/10.1002/jbm.a.34420>
42. Izadifar M, Chapman D, Babyn P, Chen X, Kelly ME. UV-assisted 3D bioprinting of nanoreinforced hybrid cardiac patch for myocardial tissue engineering. *Tissue Eng Part C Methods* **2018**; 24: 74-88. <https://doi.org/10.1089/ten.tec.2017.0346>
43. Pilato S, Moffa S, Siani G, Diomedede F, Trubiani O, Pizzicannella J, et al. 3D Graphene Oxide-Polyethylenimine Scaffolds for Cardiac Tissue Engineering. *ACS Appl Mater Interfaces* **2023**; 15: 14077-14088. <https://doi.org/10.1021/acami.3c00216>
44. Khorshidi S, Solouk A, Mirzadeh H, Mazinani S, Lagaron JM, Sharifi S, et al. A review of key challenges of electrospun scaffolds for tissue-engineering applications. *J Tissue Eng Regen Med* **2016**; 10: 715-38. <https://doi.org/10.1002/term.1978>
45. Xue Y, Ravishankar P, Zeballos MA, Sant V, Balachandran K, Sant S. Valve leaflet-inspired elastomeric scaffolds with tunable and anisotropic mechanical properties. *Polym Adv Technol* **2020**; 31: 94-106. <https://doi.org/10.1002/pat.4750>
46. Jiang T, Carbone EJ, Lo KW-H, Laurencin CT. Electrospinning of polymer nanofibers for tissue regeneration. *Prog Polym Sci* **2015**; 46: 1-24. <https://doi.org/10.1016/j.progpolymsci.2014.12.001>
47. Ding J, Zhang J, Li J, Li D, Xiao C, Xiao H, et al. Electrospun polymer biomaterials. *Prog Polym Sci* **2019**; 90: 1-34. <https://doi.org/10.1016/j.progpolymsci.2019.01.002>
48. Nazari H, Azadi S, Hatamie S, Zomorrod MS, Ashtari K, Soleimani M, et al. Fabrication of graphene-silver/polyurethane nanofibrous scaffolds for cardiac tissue engineering. *Polym Adv Technol* **2019**; 30: 2086-99.
49. Fakhrali A, Poursharifi N, Nasari M, Semnani D, Salehi H, Ghane M, et al. Fabrication and characterization of PCL/Gel nanofibrous scaffolds incorporated with graphene oxide applicable in cardiac tissue engineering. *Polymer-Plastics Technology and Materials* **2021**; 60: 2025-41.
50. Zhu J, Marchant RE. Design properties of hydrogel tissue-engineering scaffolds. *Expert Rev Med Devices* **2011**; 8: 607-26. <https://doi.org/10.1586/erd.11.27>
51. Saludas L, Pascual-Gil S, Prósper F, Garbayo E, Blanco-Prieto M. Hydrogel based approaches for cardiac tissue engineering. *Int J Pharm* **2017**; 523: 454-75. <https://doi.org/10.1016/j.ijpharm.2016.10.061>
52. Zargar SM, Mehdikhani M, Rafienia M. Reduced graphene oxide-reinforced gellan gum thermoresponsive hydrogels as a myocardial tissue engineering scaffold. *J Bioact Compat Polym* **2019**; 34: 331-45. <https://doi.org/10.1177/0883911519876080>
53. Amiryaghoubi N, Fathi M, Barar J, Omid Y. Hydrogel-based scaffolds for bone and cartilage tissue engineering and regeneration. *React Funct Polym* **2022**; 177: 105313. <https://doi.org/10.1016/j.reactfunctpolym.2022.105313>
54. Rufaihah AJ, Seliktar D. Hydrogels for therapeutic cardiovascular angiogenesis. *Adv Drug Deliv Rev* **2016**; 96: 31-9. <https://doi.org/10.1016/j.addr.2015.07.003>
55. Camci-Unal G, Annabi N, Dokmeci MR, Liao R, Khademhosseini A. Hydrogels for cardiac tissue engineering. *NPG Asia Mater* **2014**; 6: e99. <https://doi.org/10.1038/am.2014.19>
56. Walker BW, Lara RP, Mogadam E, Yu CH, Kimball W, Annabi N. Rational design of microfabricated electroconductive hydrogels for biomedical applications. *Prog Polym Sci* **2019**; 92: 135-157. <https://doi.org/10.1016/j.progpolymsci.2019.01.002>

- doi.org/10.1016/j.progpolymsci.2019.02.007
57. Talebi A, Labbaf S, Karimzadeh F, Masaeli E, Nasr Esfahani M-H. Electroconductive Graphene Containing Polymeric Patch: A Promising Platform for Cardiac Repair. *ACS Biomater Sci Eng* **2020**; 6: 4214-24. <https://doi.org/10.1021/acsbomaterials.0c00266>
  58. Ameri SK, Singh PK, Sonkusale SR. Liquid gated three dimensional graphene network transistor. *Carbon* **2014**; 79: 572-7. <https://doi.org/10.1016/j.carbon.2014.08.018>
  59. Ameri SK, Singh PK, D'Angelo AJ, Panzer MJ, Sonkusale SR. Flexible 3D Graphene Transistors with Ionogel Dielectric for Low-Voltage Operation and High Current Carrying Capacity. *Adv Electron Mater* **2016**; 2: 1500355. <https://doi.org/10.1002/aelm.201500355>
  60. Ameri S, Singh P, Sonkusale S, editors. Three dimensional monolayer graphene foam for ultra-sensitive pH sensing. *Solid-State Sensors, Actuators and Microsystems (TRANSDUCERS), 2015 Transducers-2015 18th International Conference on*; **2015**: IEEE.
  61. Jing X, Mi H-Y, Napiwocki BN, Peng X-F, Turng L-S. Mussel-inspired electroactive chitosan/graphene oxide composite hydrogel with rapid self-healing and recovery behavior for tissue engineering. *Carbon* **2017**; 125: 557-70. <https://doi.org/10.1016/j.carbon.2017.09.071>
  62. Shin SR, Zihlmann C, Akbari M, Assawes P, Cheung L, Zhang K, et al. Reduced graphene oxide-gelMA hybrid hydrogels as scaffolds for cardiac tissue engineering. *Small* **2016**; 12: 3677-89. <https://doi.org/10.1002/sml.201600178>
  63. Jiang L, Chen D, Wang Z, Zhang Z, Xia Y, Xue H, et al. Preparation of an Electrically Conductive Graphene Oxide/Chitosan Scaffold for Cardiac Tissue Engineering. *Appl Biochem Biotechnol* **2019**; 188: 952-964. <https://doi.org/10.1007/s12010-019-02967-6>
  64. Smith AS, Yoo H, Yi H, Ahn EH, Lee JH, Shao G, et al. Micro- and nano-patterned conductive graphene-PEG hybrid scaffolds for cardiac tissue engineering. *ChemComm* **2017**; 53: 7412-5. <https://doi.org/10.1039/C7CC01988B>
  65. Hibberd M, Jewell B. Calcium-and length-dependent force production in rat ventricular muscle. *J Physiol* **1982**; 329: 527-40. <https://doi.org/10.1113/jphysiol.1982.sp014317>
  66. Nazari H, Azadi S, Hatamie S, Zomorrod MS, Ashtari K, Soleimani M, et al. Fabrication of graphene-silver/polyurethane nanofibrous scaffolds for cardiac tissue engineering. *Polym Adv Technol* **2019**; 30: 2086-99. <https://doi.org/10.1002/pat.4641>
  67. Zhou J, Yang X, Liu W, Wang C, Shen Y, Zhang F, et al. Injectable OPF/graphene oxide hydrogels provide mechanical support and enhance cell electrical signaling after implantation into myocardial infarct. *Theranostics* **2018**; 8: 3317. <https://doi.org/10.7150/thno.25504>
  68. Shin SR, Aghaei-Ghareh-Bolagh B, Gao X, Nikkhah M, Jung SM, Dolatshahi-Pirouz A, et al. Layer-by-Layer Assembly of 3D Tissue Constructs with Functionalized Graphene. *Adv Funct Mater* **2014**; 24: 6136-44. <https://doi.org/10.1002/adfm.201401300>
  69. Norahan MH, Amroon M, Ghahremanzadeh R, Mahmoodi M, Baheiraei N. Electroactive graphene oxide-incorporated collagen assisting vascularization for cardiac tissue engineering. *J Biomed Mater Res A* **2019**; 107: 204-19. <https://doi.org/10.1002/jbm.a.36555>
  70. Lee T-J, Park S, Bhang SH, Yoon J-K, Jo I, Jeong G-J, et al. Graphene enhances the cardiomyogenic differentiation of human embryonic stem cells. *Biochem Biophys Res Commun* **2014**; 452: 174-80. <https://doi.org/10.1016/j.bbrc.2014.08.062>
  71. Engler AJ, Sen S, Sweeney HL, Discher DE. Matrix elasticity directs stem cell lineage specification. *Cell* **2006**; 126: 677-89. <https://doi.org/10.1016/j.cell.2006.06.044>
  72. Martino MM, Mochizuki M, Rothenfluh DA, Rempel SA, Hubbell JA, Barker TH. Controlling integrin specificity and stem cell differentiation in 2D and 3D environments through regulation of fibronectin domain stability. *Biomaterials* **2009**; 30: 1089-97. <https://doi.org/10.1016/j.biomaterials.2008.10.047>
  73. Ogura N, Kawada M, Chang W-J, Zhang Q, Lee S-Y, Kondoh T, et al. Differentiation of the human mesenchymal stem cells derived from bone marrow and enhancement of cell attachment by fibronectin. *J Oral Sci* **2004**; 46: 207-13. <https://doi.org/10.2334/josnusd.46.207>
  74. Malan D, Reppel M, Dobrowolski R, Roell W, Smyth N, Hescheler J, et al. Lack of Laminin  $\gamma$ 1 in Embryonic Stem Cell-Derived Cardiomyocytes Causes Inhomogeneous Electrical Spreading Despite Intact Differentiation and Function. *Stem Cells* **2009**; 27: 88-99. <https://doi.org/10.1634/stemcells.2008-0335>
  75. Hynes RO. Integrins: versatility, modulation, and signaling in cell adhesion. *Cell* **1992**; 69: 11-25. [https://doi.org/10.1016/0092-8674\(92\)90115-S](https://doi.org/10.1016/0092-8674(92)90115-S)
  76. Schaller MD, Hildebrand JD, Shannon JD, Fox JW, Vines RR, Parsons JT. Autophosphorylation of the focal adhesion kinase, pp125FAK, directs SH2-dependent binding of pp60src. *Mol Cell Biol* **1994**; 14: 1680-8. <https://doi.org/10.1128/mcb.14.3.1680-1688.1994>
  77. Chen H-C, Appeddu PA, Isoda H, Guan J-L. Phosphorylation of tyrosine 397 in focal adhesion kinase is required for binding phosphatidylinositol 3-kinase. *J Biol Chem* **1996**; 271: 26329-34. <https://doi.org/10.1074/jbc.271.42.26329>
  78. Poleskaya A, Seale P, Rudnicki MA. Wnt signaling induces the myogenic specification of resident CD45+ adult stem cells during muscle regeneration. *Cell* **2003**; 113: 841-52. [https://doi.org/10.1016/S0092-8674\(03\)00437-9](https://doi.org/10.1016/S0092-8674(03)00437-9)
  79. Auer M, Hausott B, Klimaschewski L. Rho GTPases as regulators of morphological neuroplasticity. *Anat Anz* **2011**; 193: 259-66. <https://doi.org/10.1016/j.aanat.2011.02.015>
  80. Ahadian S, Zhou Y, Yamada S, Estili M, Liang X, Nakajima K, et al. Graphene induces spontaneous cardiac differentiation in embryoid bodies. *Nanoscale* **2016**; 8: 7075-84. <https://doi.org/10.1039/C5NR07059G>
  81. Bahrami S, Baheiraei N, Mohseni M, Razavi M, Ghaderi A, Azizi B, et al. Three-dimensional graphene foam as a conductive scaffold for cardiac tissue engineering. *J Biomater Appl* **2019**; 0885328219839037. <https://doi.org/10.1177/0885328219839037>
  82. Park J, Park S, Ryu S, Bhang SH, Kim J, Yoon JK, et al. Graphene-regulated cardiomyogenic differentiation process of mesenchymal stem cells by enhancing the expression of extracellular matrix proteins and cell signaling molecules. *Adv Healthc Mater* **2014**; 3: 176-81. <https://doi.org/10.1002/adhm.201300177>
  83. Donaldson K, Aitken R, Tran L, Stone V, Duffin R, Forrest G, et al. Carbon nanotubes: a review of their properties in relation to pulmonary toxicology and workplace safety. *Toxicol Sci* **2006**; 92: 5-22. <https://doi.org/10.1093/toxsci/kfj130>
  84. Sasidharan A, Panchakarla LS, Sadanandan AR, Ashokan A, Chandran P, Girish CM, et al. Hemocompatibility and macrophage response of pristine and functionalized graphene. *Small* **2012**; 8: 1251-63. <https://doi.org/10.1002/sml.201102393>
  85. Syama S, Mohanan P. Safety and biocompatibility of graphene: A new generation nanomaterial for biomedical application. *Int J Biol Macromol* **2016**; 86: 546-55. <https://doi.org/10.1016/j.ijbiomac.2016.01.116>
  86. Sasidharan A, Panchakarla L, Chandran P, Menon D, Nair S, Rao C, et al. Differential nano-bio interactions and toxicity effects of pristine versus functionalized graphene. *Nanoscale* **2011**; 3: 2461-4. <https://doi.org/10.1039/C1NR10172B>
  87. Akhavan O, Ghaderi E, Akhavan A. Size-dependent genotoxicity of graphene nanoplatelets in human stem cells. *Biomaterials* **2012**; 33: 8017-25. <https://doi.org/10.1016/j.biomaterials.2012.07.040>
  88. Mu Q, Su G, Li L, Gilbertson BO, Yu LH, Zhang Q, et al. Size-dependent cell uptake of protein-coated graphene oxide nanosheets. *ACS Appl Mater Interfaces* **2012**; 4: 2259-66. <https://doi.org/10.1021/am300253c>

89. Chang Y, Yang S-T, Liu J-H, Dong E, Wang Y, Cao A, *et al.* In vitro toxicity evaluation of graphene oxide on A549 cells. *Toxicol Lett* **2011**; 200: 201-10. <https://doi.org/10.1016/j.toxlet.2010.11.016>
90. Wilczek P, Major R, Lipinska L, Lackner J, Mzyk A. Thrombogenicity and biocompatibility studies of reduced graphene oxide modified acellular pulmonary valve tissue. *Mater Sci Eng C* **2015**; 53: 310-21. <https://doi.org/10.1016/j.msec.2015.04.044>
91. Cheng L, Yang K, Shao M, Lu X, Liu Z. In vivo pharmacokinetics, long-term biodistribution and toxicology study of functionalized upconversion nanoparticles in mice. *Nanomedicine* **2011**; 6: 1327-40. <https://doi.org/10.2217/nnm.11.56>
92. Demirel E, Karaca E, Durmaz YY. Effective PEGylation method to improve biocompatibility of graphene derivatives. *Eur Polym J* **2020**; 124: 109504. <https://doi.org/10.1016/j.eurpolymj.2020.109504>
93. Xu M, Zhu J, Wang F, Xiong Y, Wu Y, Wang Q, *et al.* Improved in vitro and in vivo biocompatibility of graphene oxide through surface modification: poly (acrylic acid)-functionalization is superior to PEGylation. *ACS nano* **2016**; 10: 3267-81. <https://doi.org/10.1021/acsnano.6b00539>
94. Zhang S, Yang K, Feng L, Liu Z. In vitro and in vivo behaviors of dextran functionalized graphene. *Carbon* **2011**; 49: 4040-9. <https://doi.org/10.1016/j.carbon.2011.05.056>
95. Chowdhury SM, Fang J, Sitharaman B. Interaction of graphene nanoribbons with components of the blood vascular system. *Future Sci OA* **2015**; 1: FSO19. <https://doi.org/10.4155/fso.15.17>
96. Sivashankari B, Moorthi A, Abudhahir KM, Prabakaran M. Preparation and characterization of three-dimensional scaffolds based on hydroxypropyl chitosan-graft-graphene oxide. *Int J Biol Macromol* **2018**; 110: 522-30. <https://doi.org/10.1016/j.ijbiomac.2017.11.033>